Octave-spanning carrier-envelope phase stabilized visible pulse with sub-3-fs pulse duration

Kotaro Okamura[1,2,*] and Takayoshi Kobayashi[1,2,3,4]

[1]*Advanced Ultrafast Laser Research Center and Department of Engineering Science, University of Electro-Communications, 1-5-1 Chofugaoka, Chofu, Tokyo 182-8585, Japan*

[2]*JST, ICORP, Ultrashort Pulse Laser Project, 4-1-8 Honcho, Kawaguchi, Saitama 332-0012, Japan*

[3]*Department of Electrophysics, National Chiao-Tung University, 1001 Ta Hsueh Road, Hsinchu 3005, Taiwan*

[4]*Institute of Laser Engineering, Osaka University, 2-6 Yamada-Oka, Suita, Osaka 565-0871, Japan*

**Corresponding author: okamura@ils.uec.ac.jp*

Received November 1, 2010; accepted November 29, 2010;
posted December 15, 2010 (Doc. ID 137526); published January 12, 2011

The visible second harmonic of the idler output from a noncollinear optical parametric amplifier was compressed using adaptive dispersion control with a deformable mirror. The amplifier was pumped by and seeded in the signal path by a common 400 nm second-harmonic pulse from a Ti:sapphire regenerative amplifier. Thus, both the idler output and the second harmonic of the idler were passively carrier-envelope phase stabilized. The shortest pulse duration achieved was below 3 fs. © 2011 Optical Society of America

OCIS codes: 140.3515, 140.7090, 190.4410, 190.7110, 320.5520.

The ability to generate isolated ultrashort pulses with a broad spectrum in the visible region is important for many applications. For example, pump–probe experiments that can resolve molecular vibrations became possible with the development of sub-5-fs noncollinear optical parametric amplifiers (NOPAs) [1–8]. These experiments shed light on many ultrafast photophysical processes, such as exciton self-trapping [9] and breather–soliton formation [10], and photochemical processes such as the transitional states during isomerization in bacteriorhodopsin [11] and Claisen rearrangement [12].

Recently, there have been several reports on the synthesis of short or arbitrary optical pulse trains from Raman sidebands generated by molecular modulation in H_2 [13,14]. Even sub-single-cycle optical pulses have been synthesized from seven sidebands in the near-UV-to-near-IR region [14]. However, because the time between pulses is too short (<100 fs) and their extremely high repetition rates prohibit downsampling, these pulses are of little use for investigating chemical or photochemical processes, which typically have time scales of >100 fs.

To our knowledge, the shortest isolated pulse that has been generated in the visible region is a 2.6 fs pulse produced by Matsubara *et al.* [15]. It was generated by spectral broadening in a hollow fiber and dispersion compensation using a spatial light modulator in a 4-*f* setup. However, because their output pulse spectrum contained very complicated fine structures that are unsuitable for spectroscopy, it has not been used in any spectroscopic applications. In wavelength regions longer than the visible, the shortest pulse is a 4.3 fs pulse produced by our group [16] by compressing from a NOPA idler. The present study is an extension of this work to generate a carrier-envelope phase (CEP) stabilized sub-3-fs pulse.

The sub-3-fs pulse is based on a NOPA with a 1-mm-thick β – BaB_2O_4 crystal (BBO) as the gain medium and pumped by the 400 nm second harmonic (width, 70 fs; repetition rate, 5 kHz; energy, 20 μJ; radius, 50 μm) of a Ti:sapphire regenerative amplifier. As shown in Fig. 1(a), the seed of the NOPA is the supercontinuum generated in a CaF_2 plate from a fraction (0.6 μJ) of the 400 nm pulse and is injected as the signal, the higher-frequency wave of the parametric amplification. Because the pump and the signal have the same CEPs, the CEP of the newly generated lower-frequency idler (energy of ~0.5 μJ), which is generated as the difference frequency between the pump and the signal, is passively stabilized [17]. With slow (~1 s) feedback control to suppress drift, the idler CEP of this system is stable enough to perform optical poling experiments of a few hours [18,19].

The idler output with an octave-spanning (800 nm–1.6 μm) spectrum has an angular dispersion of 170 μrad/nm, which is similar to the variation in the phase-matching angle with wavelength for second-harmonic generation of the idler in the NOPA BBO. The quasi-satisfactory condition for angularly dispersed achromatic phase-matched frequency doubling [20–22] leads to a considerable amount of the idler second harmonic (idler-SH) generated overlapping onto the idler beam (with different polarization: idler, vertical; idler-SH, horizontal). As shown in Fig. 1(b), the wavelength range of the idler-SH is 430–800 nm (i.e., a frequency width of >300 THz).

Figure 2 shows the optical layout used for compensating the angular and group-delay dispersion. We first

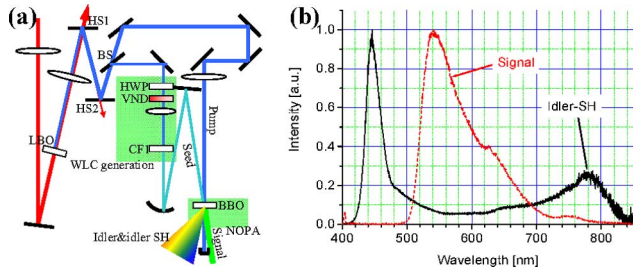

Fig. 1. (Color online) (a) Schematic of NOPA: LBO, LiB_3O_5 crystal for second-harmonic generation; HS, harmonic separator; BS, beam splitter; HWP, half-wave plate; VND, variable neutral-density filter; CF1, calcium fluoride crystal for white-light continuum generation; BBO, β – BaB_2O_4 crystal for parametric amplification. (b) Spectra of idler-SH (solid black curve) and signal (broken red curve).

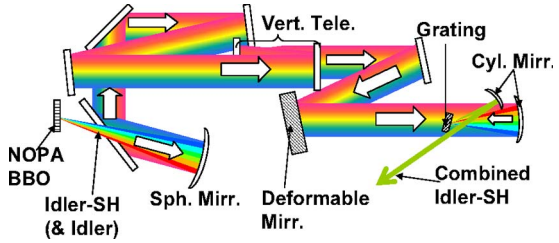

Fig. 2. (Color online) Setup for angular and group-delay dispersion compensation. Sph. Mirr., spherical mirror for collimation; Vert. Tele., telescope for reducing vertical beam width; Cyl. Mirr., cylindrical mirrors for focusing onto grating and collimating after beam combination.

collimated the diverging fan-shaped idler-SH beam by using a spherical mirror, thereby converting the large angular dispersion into spatial dispersion. The collimated idler-SH with spatial dispersion was then reflected from a deformable mirror [(DM) Flexible Optical] for high-order group-delay dispersion control. Finally, the spatial dispersion of the idler-SH was converted back into angular dispersion by reflection from a cylindrical mirror and it was compensated by the diffraction with the grating.

After adjusting the beam size, the whole idler-SH beam was characterized with a sum-frequency-generation (SFG) cross-correlation frequency-resolved optical gating (XFROG) [23,24] using a 800 nm reference pulse. Compared with SHG-FROG pulse diagnostics [25], a SFG-XFROG can characterize lower energy pulses by employing strong reference pulses; it also requires narrower frequency-conversion bandwidths [26].

An 800 nm reference pulse was split from the same 800 nm regenerative amplifier output that was used to drive the NOPA. It was compressed to 45 fs FWHM using a dual-prism pair and characterized by SHG-FROG using a Michelson interferometer and the same optical setup as described in the following.

To avoid geometric smearing in the SFG process, the idler-SH and 800 nm reference pulses were overlapped using a chromium-coated partial mirror and focused by an off-axis parabolic mirror (OAP) onto a 10-μm-thick BBO for a SFG-FROG. The BBO thickness was measured independently. Because the CEP of the 800 nm reference beam varies randomly and that of the idler-SH is passively stabilized, interference between them is washed out when integrated over 8000 shots.

Because the idler-SH and 800 nm reference beams were collinearly incident on the XFROG-BBO, the generated SFG-XFROG signal, the second harmonic of the 800 nm reference beam (ref-SH), the idler-SH beam, and the intense 800 nm reference beam were all collinear with each other. After collimation (i.e., refocusing) by an OAP, the SFG-XFROG signal was filtered in two steps. First, a Glan–Thompson prism was used to transmit a vertically polarized SFG-XFROG signal and ref-SH. Second, a fused-silica prism was used for spectral filtering as follows. The beam spectrally dispersed by the prism was reflected back by a spherical mirror and retransmitted through the same prism so that it was recollimated. Because the residual idler-SH and 800 nm reference beams have longer wavelengths than the other beams, they could be completely removed by placing a beam block near the surface of the spherical mirror. The OAP after the XFROG-BBO was adjusted so that the refocused beam was precisely focused on the surface of the spherical mirror. The double-filtered SFG-XFROG signal beam was refocused by another OAP onto the fiber input of a spectrometer (Ocean Optics, USB4000). Although the above two-step filtering did not reduce the intensity of ref-SH, its intensity was sufficiently stable that we could remove it by simply subtracting the background, which was obtained immediately before and after the measurement.

A fused-silica wedge was inserted for low-order dispersion control. Fine dispersion control was achieved using the DM, which is an electrostatically driven membrane with 19 electrodes.

Note that, in XFROG measurements with a reference beam with a much narrower spectrum than the pulse being measured (idler-SH), the group delay of the idler-SH pulse at some wavelength can be directly estimated without retrieval from the XFROG trace by simply calculating the peak position (assuming a clean reference pulse) in the delay time for the corresponding spectral pixel of the spectrometer.

The following feedback procedure was used. First we obtained a SFG-XFROG trace by setting the DM electrode voltages to the middle of their driving ranges. Second, we obtained 19 sets of traces by individually maximizing each of the DM electrode voltages. Using these sets of data, we tracked the group delay as a function of wavelength, compared 19 driven group-delay spectra with the nondriven group-delay spectrum, and obtained a calibration curve for the group delay as a function of the electrode voltage. The total group-delay variation was assumed to be a linear combination of each electrode drive, and we iteratively minimized the group-delay deviation using the calibration curve.

Figures 3(a) and 3(b) respectively show measured and retrieved XFROG traces. Figures 4(a) and 4(b) show the retrieved spectrum and pulse shape along with their phases, respectively. These figures also show the spectrum measured by the spectrometer and the transform-limited (TL) pulse shape calculated from the retrieved spectrum. The measured and retrieved spectra agree well with each other. The temporal FWHM of the retrieved pulse was 2.4 fs, which is close to the TL pulse width of 2.2 fs.

In summary, we have demonstrated compression of CEP-stabilized NOPA second-harmonic visible–NIR output down to 2.4 fs. The total energy of the compressed idler-SH pulse was around 1 nJ, and the energy fraction of the main pulse was 47%. The output spectrum

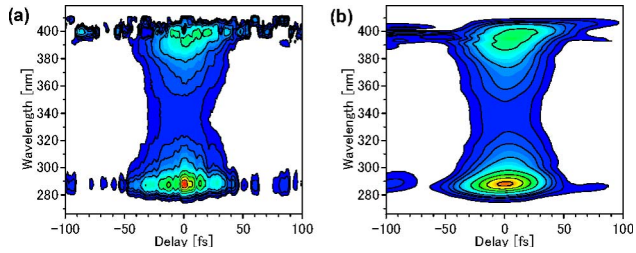

Fig. 3. (Color online) (a) SFG-XFROG trace of idler-SH and (b) retrieved trace.

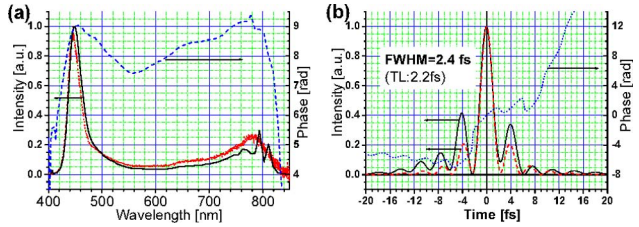

Fig. 4. (Color online) (a) Retrieved and measured spectral pulse shape (solid black curve, retrieved intensity; dotted red curve, measured intensity; broken blue curve, retrieved phase). (b) Retrieved temporal pulse shape (solid black curve, retrieved intensity; dotted blue curve, retrieved phase; broken red curve, intensity of TL pulse).

was smooth, making it suitable for spectroscopic applications.

While the energy of the compressed idler-SH pulse is a little too low for the pulse to be used as the pump in pump–probe experiments, there is a higher energy (~1 μJ) signal beam from the same NOPA [its spectrum is shown in Fig. 1(b)]. Because the signal beam has no appreciable angular dispersion and its spectrum is sufficiently wide to support a pulse duration of 6 fs, compression using the conventional combination of a negatively chirped mirror pair and a prism pair and use as the pump beam in a pump–probe experiment are feasible. The idler-SH pulse can be used as a wide-spectrum probe beam in such an experiment.

Because the idler-SH and idler pulses are both CEP stable and simultaneously generated in the same BBO, synthesis of phase-stable pulse by their combination is feasible. Their polarizations can be aligned using a periscope. With a combined wavelength range of 430 nm – 1.6 μm, this approach has the potential to realize a near-two-octave sub 2 fs pulse.

References

1. G. Cerullo, M. Nisoli, S. Stagira, and S. De Silvestri, Opt. Lett. **23**, 1283 (1998).
2. A. Shirakawa and T. Kobayashi, Appl. Phys. Lett. **72**, 147 (1998).
3. A. Shirakawa, I. Sakane, and T. Kobayashi, Opt. Lett. **23**, 1292 (1998).
4. E. Riedle, M. Beutter, S. Lochbrunner, J. Piel, S. Schenkl, S. Spoerlein, and W. Zinth, Appl. Phys. B **71**, 457 (2000).
5. T. Kobayashi and A. Shirakawa, Appl. Phys. B **70**, 389 (2000).
6. M. Zavelani-Rossi, G. Cerullo, S. De Silvestri, L. Gallmann, N. Matuschek, G. Steinmeyer, U. Keller, G. Angelow, V. Scheuer, and T. Tschudi, Opt. Lett. **26**, 1155 (2001).
7. A. Baltuška, T. Fuji, and T. Kobayashi, Opt. Lett. **27**, 306 (2002).
8. A. Baltuška and T. Kobayashi, Appl. Phys. B **75**, 427 (2002).
9. A. Sugita, T. Saito, H. Kano, M. Yamashita, and T. Kobayashi, Phys. Rev. Lett. **86**, 2158 (2001).
10. S. Adachi, V. M. Kobryanskii, and T. Kobayashi, Phys. Rev. Lett. **89**, 027401 (2002).
11. T. Kobayashi, T. Saito, and H. Ohtani, Nature **414**, 531 (2001).
12. I. Iwakura, A. Yabushita, and T. Kobayashi, Chem. Lett. **39**, 374 (2010).
13. M. Y. Shverdin, D. R. Walker, D. D. Yavuz, G. Y. Yin, and S. E. Harris, Phys. Rev. Lett. **94**, 033904 (2005).
14. W. J. Chen, Z.-M. Hsieh, S. W. Huang, H. Y. Su, C. J. Lai, T. T. Tang, C. H. Lin, C. K. Lee, R. P. Pan, C. L. Pan, and A. H. Kung, Phys. Rev. Lett. **100**, 163906 (2008).
15. E. Matsubara, K. Yamane, T. Sekikawa, and M. Yamashita, J. Opt. Soc. Am. B **24**, 985 (2007).
16. S. Adachi, P. Kumbhakar, and T. Kobayashi, Opt. Lett. **29**, 1150 (2004).
17. A. Baltuška, T. Fuji, and T. Kobayashi, Phys. Rev. Lett. **88**, 133901 (2002).
18. S. Adachi and T. Kobayashi, Phys. Rev. Lett. **94**, 153903 (2005).
19. K. Okamura and T. Kobayashi, Opt. Commun. **281**, 5870 (2008).
20. S. Saikan, D. Ouw, and F. P. Schäfer, Appl. Opt. **18**, 193 (1979).
21. G. Szabó and Z. Bor, Appl. Phys. B **50**, 51 (1990).
22. T. Kanai, X. Zhou, T. Sekikawa, S. Watanabe, and T. Togashi, Opt. Lett. **28**, 1484 (2003).
23. S. Linden, H. Giessen, and J. Kuhl, Phys. Status Solidi B **206**, 119 (1998).
24. S. Linden, J. Kuhl, and H. Giessen, Opt. Lett. **24**, 569 (1999).
25. R. Trebino and D. J. Kane, J. Opt. Soc. Am. A **10**, 1101 (1993).
26. A. Baltuška, M. S. Pshenichnikov, D. A. Wiersma, and R. Szipocs, in *Ultrafast Processes in Spectroscopy*, R. Kaarli, A. Freiberg, and P. Saari, eds. (Institute of Physics, University of Tartu, 1998), p. 7.